Indian Journal of Pure & Applied Physics
Vol. 61, August 2023, pp. 671-682
DOI: 10.56042/ijpap.v61i8.1240

# Mid-winter Stratospheric Warming Effects on Tropical Convection over the Indian Sector: Case Studies

G J Bhagavathiammal

Department of Medical Physics, Centre for Climate Change and Disaster Management, Anna University, College of Engineering Guindy, Sardar Patel Road, Guindy, Chennai-600 025, Tamil Nadu, India

*Received 8 May 2023; accepted 18 July 2023*

The present study investigates the impact of northern mid-winter major stratospheric warming on tropical convection over the Indian region by examining the five Mid-winter Major Stratospheric Warming (MSW) events 2003/04, 2005/06, 2008/09, 2012/13, and 2018/19. The dynamical variables like temperature, wind components, and Outgoing Longwave Radiation are utilized from ECMWF ERA-Interim Reanalysis and NOAA site. Eliassen Palm (E-P) flux is used to visualize the upward and equator-ward propagation of extratropical Planetary Waves (PWs) from the lower atmosphere and their reach to the tropical region. The dominance of extratropical PW forcing from high to low latitudes is seen in all mid-winter cases. Further, the transfer of PW energy to low latitudes modifies the convection pattern over the Indian region. The author found depleted convection in the latitude band -15-20°N for the MSW 2003/04 and 2018/19, with frequent changes seen during MSW 2012/13 and 2005/06. On the other hand, the MSW 2008/09 show enhanced convection in the entire latitude band 20°S-20°N. This work suggests that the modification of OLR depends on the PW energy, onset time, peak temperature, and wind-reversed state during MSW.

**Keywords:** Tropical Convection; Stratospheric Warming; Outgoing Longwave Radiation

## 1 Introduction

Mid-winter Stratospheric Warming (MSW) is a remarkable stratospheric dynamical process that causes a sudden increase in polar temperature associated with the mean flow reversal. The mechanism for sudden stratospheric warming was first proposed by Matsuno[1], suggesting that the interaction of upward propagating planetary waves with the mean flow could be the reason for the sudden warming in the stratosphere[2,3]. The impact of extratropical dynamics on tropical weather is a spectacular part of the middle atmosphere[4-10]. In addition, the convergence of planetary wave fluxes drives the poleward meridional circulation, further inducing an upward motion over the tropics and a downward motion in high latitudes[11]. Many research studies have investigated the influence of SSWs on the Tropical Tropopause Layer[9,12-15]. These studies established that tropical upwelling during SSW leads to cooling in the tropical upper troposphere-lower stratosphere.

Convection is a vibrant dynamical aspect of the tropical atmosphere. A few studies reported the association between sudden stratospheric warming and tropical convection. Kodera and Yamada[16] analyzed the impact of stratospheric warming on Hadley circulation, Their study suggests the strong polar downwelling equatorial upwelling and the shift in tropical convective activity towards the southern hemisphere. A composite analysis of 12 stratospheric warming events by Kodera[9] found that decrease (increase) in convective activity over the equatorial northern (southern) hemisphere. Kuroda[17] pointed out the enhanced convection in the southern (northern) hemisphere after the occurrence of stratospheric warming (vortex intensification).

Further, the study revealed the connection between the polar and subtropical effects through direct and indirect propagation of planetary waves associated with stratospheric warming or vortex intensification. In 2011, Sridharan and Sathishkumar[18] found enhanced deep convection connected with stratospheric warming events 2003/04 and 2005/06. Furthermore, their work revealed that Potential vorticity originating from high latitudes moves toward the equator and converges in the latitude band 90°-150°E.

Though some studies have investigated the association between stratospheric warming and tropical dynamics, the bonding between stratospheric warming and equatorial dynamical processes is still imprecise. The present work will address MSW forced variability

*Corresponding authors: (E-mail: selvigjb@gmail.com)

on equatorial convection over the Indian region by utilizing case studies 2003/04, 2005/06, 2008/09, 2012/13 and 2018/19 winters.

## 2 Data Used & Methodology

### 2.1 ECMWF ERA-Interim data

ECMWF ERA-Interim is an upgraded four-dimensional assimilation system extensively utilized by many authors[8,19]. The variables such as temperature, potential vorticity, geopotential and wind components are achieved from http://data-portal.ecmwf.int/data/d/interim_daily/. These data have a spatial resolution of $1.5^o \times 1.5^o$ for 37 pressure levels from ground to 1hPa. Potential vorticity is a measure of the capacity for air to rotate in the atmosphere. It helps to understand the atmosphere's dynamic processes through ascending or descending air flows and the development or weakening of weather systems. The unit of potential vorticity is $Km^2kg^{-1}\ s^{-1}$.

### 2.2 Total Precipitation from IMDAA Reanalysis

Hourly "Total Precipitation" is retrieved from IMDAA reanalysis[20], which is a high-resolution (12km) regional reanalysis of India, operated by the National Centre for Medium-Range Weather Forecasting (NCMRWF), a centre of Excellence in weather and climate Modelling under the Ministry of Earth Sciences, Govt of India. It can be accessed through the webpage. https://rds.ncmrwf.gov.in/ .

### 2.3 Outgoing Longwave Radiation (OLR) & Precipitation data

Interpolated daily Outgoing Longwave Radiation (OLR) and Precipitation are used as a proxy for tropical convection and obtained from the Climate Diagnostic Center (CDC) of the National Oceanic and Atmospheric Administration (NOAA) Satellite and NASA Tropical Rainfall Measurement Mission (TRMM). A complete description of the (interpolated) OLR dataset was given by Liebermann and Smith[21]. The data presented here are smoothed using a 5-day running average.

### 2.4 Eliassen Palm (E-P) flux diagnostics:

The traditional diagnostic tool "Eliassen Palm (E-P) flux" has been used to visualize planetary wave forcing/ breaking during sudden stratospheric warming. Numerous authors have explored the middle atmospheric dynamical processes using Eliassen-Palm flux since the 1960s[9, 19, 22-27]. E-P flux and its divergence are calculated using the following equations in spherical coordinates [24].

$$F^{(\phi)} = \rho_o a \cos\phi \left( \overline{u}_z \frac{\overline{v'\theta'}}{\overline{\theta}_z} - \overline{u'v'} \right) \quad \ldots (1)$$

$$F^{(z)} = \rho_o a \cos\phi \times \left\{ \left[ f - (a\cos\phi)^{-1} \left( \overline{u}\cos\phi \right)_\phi \right] \frac{\overline{v'\theta'}}{\overline{\theta}_z} - \overline{u'w'} \right\} \quad \ldots (2)$$

$$\nabla . F = (a\cos\phi)^{-1} \frac{\partial}{\partial\phi} \left( F^{(\phi)} \cos\phi \right) + \frac{\partial}{\partial z} F^{(z)} \quad \ldots (3)$$

$$D = \frac{1}{\rho_o a \cos\phi} \nabla . F \quad \ldots (4)$$

The above equations are denoted by the standard notation of Andrews *et al*. (1987). The primes and overbars represent the zonal mean and deviations from the zonal mean, respectively. Subscripts φ and z means the derivative concerning the meridional and vertical coordinate. The orientation of E-P flux vectors indicates the propagation direction of planetary waves. The notation $.F$ represents the wave-induced torque per unit volume acting on the mean flow. Negative (positive) E-P flux divergence represents the strong convergence (divergence) of wave forcing.

## 3 Results

### 3.1 MSW 2003/04

Figure 1 depicts the (a) Temperature difference 90-60°N and zonal mean zonal wind at 60°N (b) Time- altitude cross-section of vertical heat flux F(z)(Kg $s^{-2}$) averaged over 60-80°N (c) Latitudinal cross-section of wave driving (d) Time –altitude cross-section of vertical heat flux F(z) averaged over low latitude 10-30°N (e) Temporal variation of OLR for the zonal mean and 60-100°E longitude averaged over the latitude band 0-5°N, 0-10°N (f) Time-Latitude distribution of potential vorticity ($Km^2kg^{-1}\ s^{-1}$) averaged over 60-100°E at 10mb (g) Time-latitude distribution of zonal wind ($ms^{-1}$) averaged over 60-100°E at 10mb for the 90 days from 01 December 2003. Fig. 1(a) reveals that sudden warming starts on 15 December 2003 (day no.15) and attains a maximum temperature difference of about 55K on 28 December 2003 (day no:28). This warming pulse persists for about 47 days with decreasing temperature after 28 December 2003. Meanwhile, the zonal mean zonal wind at 60°N reversed around 04 January 2004 (day no: 35). Eliassen Palm flux is the prime diagnostic tool for wave propagation and wave mean flow interaction, particularly

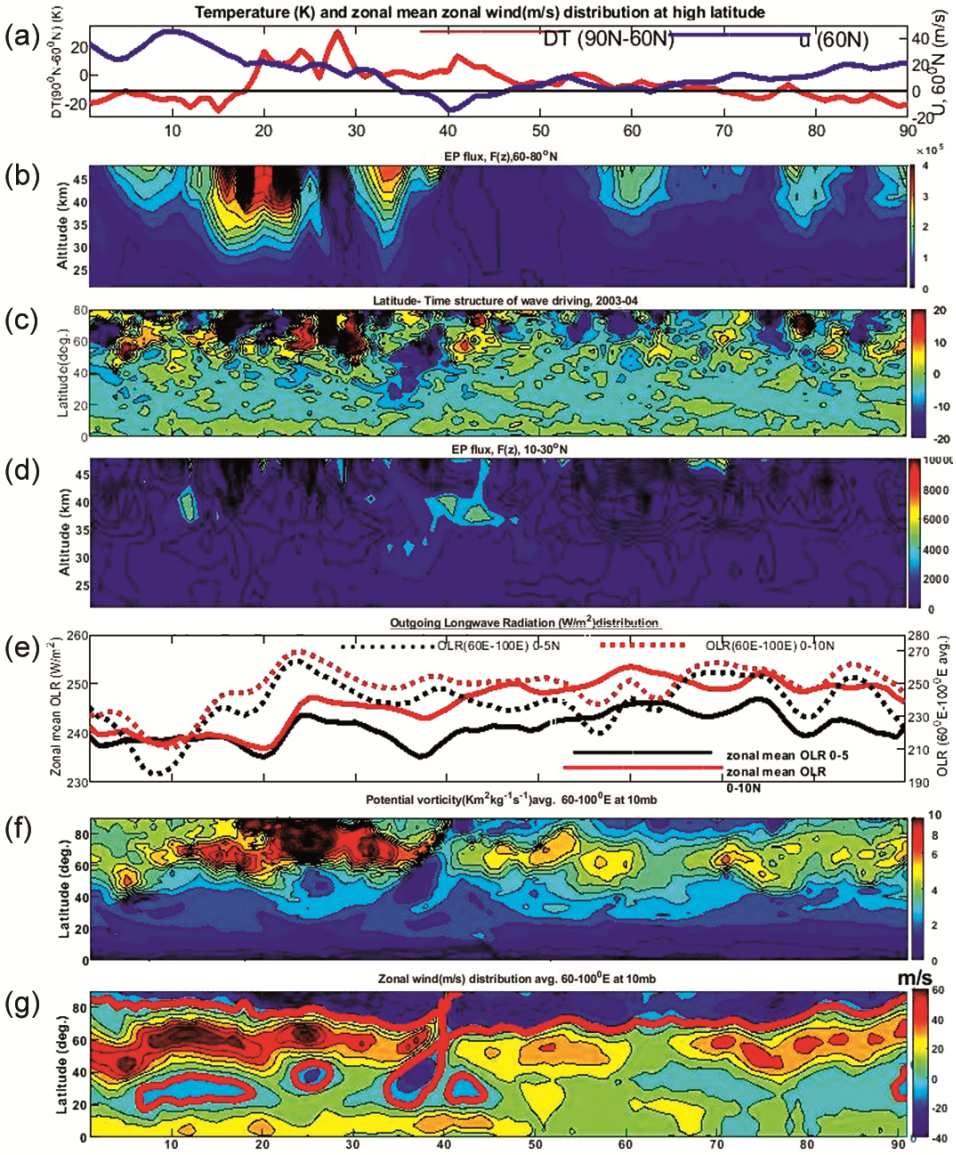


Fig. 1 — (a) Temperature difference (K) 90-60°N and zonal mean zonal wind (m/s) at 60°N (b)Time-Altitude cross-section of vertical heat flux F(z), ($Kgs^{-2}$) averaged over 60-80°N (c) averaged over low latitude 10-30°N (d) Latitudinal cross-section of wave driving ($ms^{-1}day^{-1}$) (e) Temporal variation of zonal mean and 60-100°E averaged OLR for the latitude band 0-5°N, 0-10°N (f) Time- Latitude distribution of potential vorticity ($Km^2kg^{-1}$ $s^{-1}$) averaged over 60-100°E at 10mb (g) zonal wind averaged over 60-100°E at 10mb for the winter 2003-04 (90days, 01 December 2003-28 February 2004).

stratosphere–troposphere coupling. EP flux vector shows the direction of propagation of planetary waves. EP flux divergence represents the acceleration or deceleration of zonal mean zonal wind by planetary wave forcing[22,23]. From Fig. 1(b), the heat flux distribution over the polar region (60-80°N) suggests that intense heat flux appeared in the upper stratosphere on 12 December 2003. Signatures of this heat flux were observed at the lower stratosphere on 16 December 2003 and persisted till 24 December 2003. We found additional heat flux energy between 30 December 2003- 06 January 2004 (day no. 30-38) in the middle and lower stratosphere. These flux energies observed at polar latitudes propagate meridionally and vertically downward. Latitude-time structure of wave forcing from Fig. 1(c) reveals that the confined Negative E-P flux divergence ($\nabla . F < 0$) dominates in the extra-tropics throughout the December month, which indicates the piling up of planetary wave activity. Strong convergence of wave

forcing propagated downward on 30 December 2003 (day no: 30) and reached the tropics on 03 January 2004 (day no: 34). From Fig. 1(d), we can see the entrance of heat flux energy into low latitude lower stratosphere on 03 January 2004 (day no: 34), and it persists till 19 January 2004 (day no: 50). From Fig. 1(e), the zonal mean OLR profile shows two consecutive dips on 20 December 2003 (day no: 20) and 06 January 2004 (day no: 37). The reach of extratropical heat flux at the lower stratosphere develops a drop in OLR on 20 December 2003. The OLR drop on 06 January 2004 indicates the extent of heat flux/wave forcing on low latitude lower stratosphere. However, during MSW, the OLR averaged over the Indian region (60-100°E) shows an increased OLR of about 270W/m$^2$ on 24 December 2003. High OLR informs the low and warm clouds, which are presumed to be associated with decreased convection. Fig. 1(f) shows a robust potential vorticity distribution in extratropics throughout December. The depletion of potential vorticity distribution is observed at MSW around 06 January 2004 (day no.37). This occupancy of weak potential vorticity exists in the polar region till 10 January 2004 (day no: 41). From Fig. 1(g) latitude time cross-section of zonal wind distribution (averaged 60-100°E) depicts the appearance of westward wind at high latitudes on 08 January 2004 (day no:39), which propagate meridionally downward reaches up to ~17°N. The downward propagating westward wind covers the low-latitude region from 30 December 2003 to 15 January 2004 (day no: 30-46). But, the weak eastward wind dominates near the equator.

### 3.2 MSW 2005/06

Figure 2 describes the stratospheric status during the winter of 2005/06. Fig. 2 depicts the (a) Temperature difference (K) 90-60°N, and zonal mean zonal wind (m/s) at 60°N (b) Time-altitude cross-section of vertical heat flux F(z) averaged

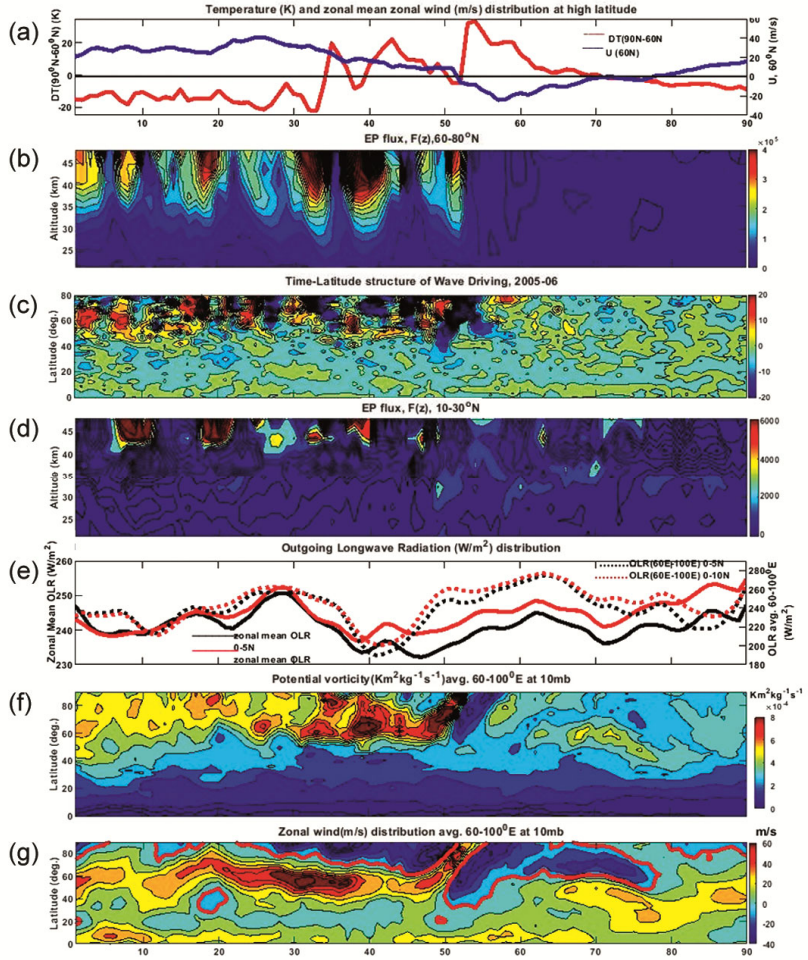


Fig. 2 — The same parameters as Figure 1 but for the 90 days of winter 2005/06 from 01 December 2005.

over 60-80°N (c) Latitudinal cross-section of wave driving (d) Time –altitude cross-section of vertical heat flux F(z) ($Kgs^{-2}$) averaged over low latitude 10-30°N (e) Temporal variation of OLR averaged over zonal mean and longitude average 60-100°E for the latitude band 0-5°N, 0-10°N (f) Time- Latitude distribution of potential vorticity ($Km^2kg^{-1}$ $s^{-1}$) averaged over 60-100°E at 10mb (g) Time-latitude distribution of zonal wind at 10mb averaged over 60-100°E for the 90 days from 01 December 2005. Fig. 2(a) reveals that sudden warming started on 02 January 2006 (day no.33). A progression of three bursts of temperature rises and attains a maximum temperature difference of about 55K on 23 January 2006 (day no:54). This warming pulses persist for about a month with decreasing temperature after 23 January 2006. Meanwhile, the zonal mean zonal wind at 60°N reversed on 21 January 2006 (day no: 52). From Fig. 2(b), The heat flux distribution over the polar region (60-80°N) suggests that intense heat flux appears in the upper stratosphere throughout December month. In association with temperature increase, the appearance of three bursts of heat flux at high latitudes in the January month reaches the lower stratosphere on 04, 11, and 23 January 2006 (day no. 35, 42, 54). The meridional section of wave forcing from Fig. 2(c) depicts the strong convergence and divergence of planetary wave forcing in December. In connection with three heat flux bursts, wave driving also shows forceful convergence of E-P flux divergence, propagating meridionally and vertically downward. Fig. 2(d) visualizes the reach of heat flux energy at low latitudes (10-30°N). In December month, vertical downward propagation of heat flux energy is confined in the upper stratosphere. On 18 January 2006 (day no:49), Strong admittance of heat flux energy at low latitude lower stratosphere. Following this, another strong entry of heat flux energy reached the tropics on 29 January 2006, 16 February 2006, and 23 February 2006 (day no: 60, 78, and 85). Fig. 2 (e) shows the OLR variation for the zonal mean and averaged over the Indian region 60-100°E for the latitude band 0-5°N and 0-10°N. The OLR averaged over the Indian region shows a sharp drop on 11 January 2006 (day no.42), a week before the heat flux reached low latitudes (day no: 49), Whereas the zonal mean OLR shows a slight dip on 22 December 2006, referring to the reach of heat flux energy at low latitude lower stratosphere. The zonal mean OLR starts decreases on 30 December 2005 and further declined and reached the minimum on 06 January 2006 (day no: 46). Besides, a second zonal mean OLR decrease was noted on 10 February 2006 (day no: 72) on connection with heat flux energy observed at tropics. Low potential vorticity pointed downward and propagated from the upper to lower stratosphere on 19 January 2006 (day no: 50). At the time of sudden warming, the low latitude lower stratosphere was dominated by weak potential vorticity. Fig. 2(g) describes the time–latitude cross-section of zonal wind averaged over 60-100°E at 10mb. Downward descending westward wind propagates and reaches the tropics, but weak eastward wind dominates near the equator.

### 3.3 MSW 2008/09

Figure 3 is the same as Figs 1 & 2 but for winter 2008/09. Figure 3 depicts the (a) Temperature difference (K) 90-60°N and zonal mean zonal wind (m/s) at 60°N (b)Time- Altitude cross-section of vertical heat flux F(z) averaged over 60-80°N (c) Time –altitude cross-section of vertical heat flux F(z) averaged over low latitude 10-30°N (d) Latitudinal cross-section of wave driving (e) Temporal variation of OLR for zonally averaged and over 60-100°E for the latitude band 0-5°N, 0-10°N (f) Time- Latitude distribution of potential vorticity averaged over 60-100°E at 10mb (g) Time-latitude distribution of zonal wind averaged over 60-100°E at 10mb for the 90 days from 01 December 2008. A sharp temperature increase (ΔT, 90-60°N) starts on 18 January 2009 (day no: 49) and reaches a maximum rise of 45K on 23 January 2009 (day no: 54). The eastward wind reversed to the westward on 24 January 2009 (day no: 55). Recovery from westward to eastward occurs at the end of February around day no. 85. Enhanced planetary wave activity was observed in December month. Fig. 3(b) depicts the appearance of intense heat flux at high latitudes during warming. The E-P flux over the low latitude band from Fig. 3(c) reveals the reach of heat flux to the lower stratosphere with a delay of 7 days. Fig. 3(d) describes the intense converging planetary wave energy from polar to equatorial latitudes. Fig. 3(e) depicts a sharp descent of OLR in both zonal mean and longitude 60-100°E profiles, explicitly the enhanced convective activity. We can infer from Fig. 3(f) that distinct potential vorticity with downward propagation was found at the time of warming. The zonal wind structure averaged over 60-100°E from Fig. 3(g) shows the abnormal

pattern of occupancy of the westward wind both at polar and tropical latitudes. Also, the uplift (down lift) of westward wind can be observed in low (polar) latitudes at the time of sudden warming.

### 3.4 MSW 2012/13

Figure 4 describes the stratosphere's status during the winter of 2012/13. Fig. 4 depicts the (a) Temperature difference (K) 90-60°N and zonal mean

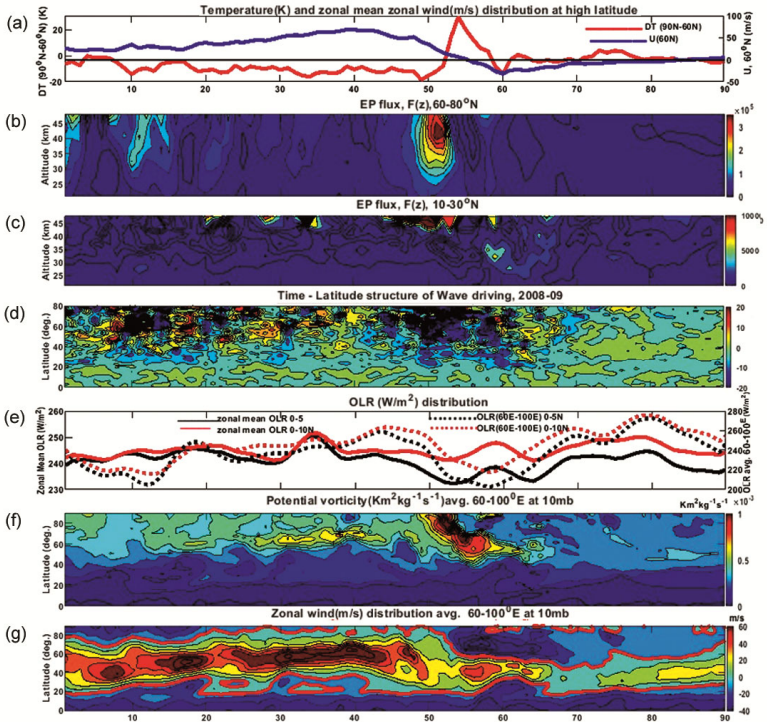


Fig. 3 — The same parameters as Figure 1 & 2 but for the 90 days of winter 2008/09 from 01 December 2008.

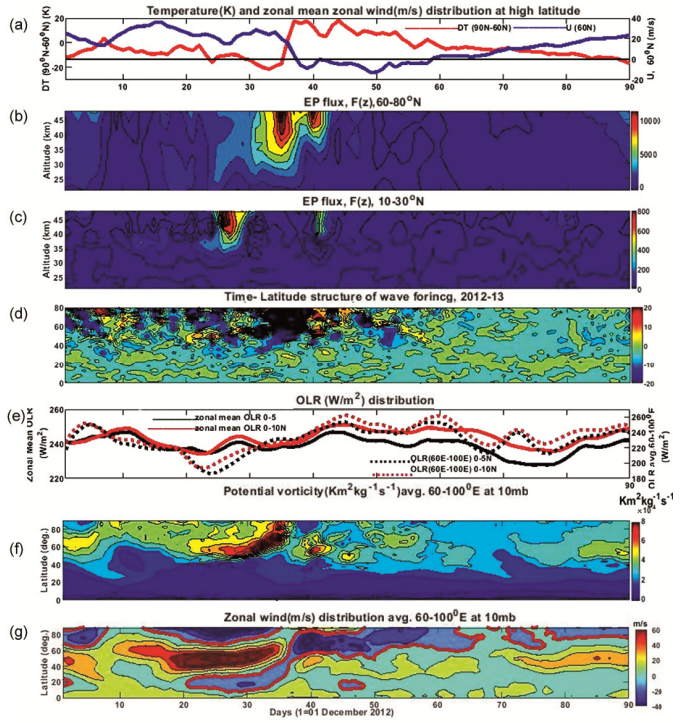


Fig. 4 — The same parameters as Figure 1 but for the 90 days of winter 2012/13 from 01 December 2012. .

zonal wind (m/s) at 60°N (b)Time-Altitude cross-section of vertical heat flux F(z) ($Kgs^{-2}$) averaged over 60-80°N (c) Latitudinal cross-section of wave driving (d) Time –altitude cross-section of vertical heat flux F(z) averaged over low latitude 10-30°N (e) Temporal variation of zonal mean OLR and over longitude average 60-100°E for the latitude 0-5°N, 0-10°N (f) Time- Latitude distribution of potential vorticity averaged over 60-100°E at 10mb (g) Time-latitude distribution of zonal wind averaged over 60-100°E at 10mb for the winter 2012-13 (90days, 01 December 2012-28 February 2013). Fig. 2(a) depicts the peak temperature that occurs on 07, 09, and 14 January 2013 (day number 37, 39, and 44), and the maximum temperature difference (ΔT) rise of 40K happens in winter 2012/13. From Fig. 2(b), zonal mean zonal wind reversed to westward on 08 January 2013 (day number: 38) during the same time as the polar temperature maximized. The zonal mean wind returned to normal conditions on 29 January 2013 (day number: 59). The temporal variation of zonal OLR averaged over 0-10°N, and 0-5°N shows a maximum dip in OLR of about 225 $W/m^2$ on 04 February and 15 February 2013. The OLR averaged over the Indian region describes a major decrease of OLR of about 190 $W/m^2$ found on 25 December 2012, almost 12 days before warming. The maximum value of potential vorticity was found between 30 December 2012 and 10 January 2013 over the Indian region, reaching up to 50°N. On 10 December 2012, the intrusion of potential vorticity reached up to 20°N.

### 3.5 MSW 2018/19

Figure 5 illustrates the stratosphere's status during winter 2018/19. Fig. 5 depicts (a) Temperature difference (K) 90-60°N and zonal mean zonal wind (m/s) at 60°N (b) Time –altitude cross-section of vertical heat flux F(z) averaged over 60-80°N (c) Time- altitude cross-section of vertical heat flux averaged over 10-30N (d) Latitudinal cross-section of wave driving (e) Temporal variation of precipitation averaged over zonal and over longitude 60-100°E at 10mb (g) Time-latitude distribution of zonal wind averaged over 60-100°E at 10mb for winter 2018/19 (90 days, 01 December 2018- 28 February 2019). The sudden warming started to rise on 23 December 2018 from -28K, and the maximum temperature reached about ~31K on 29 December 2018. The temperature

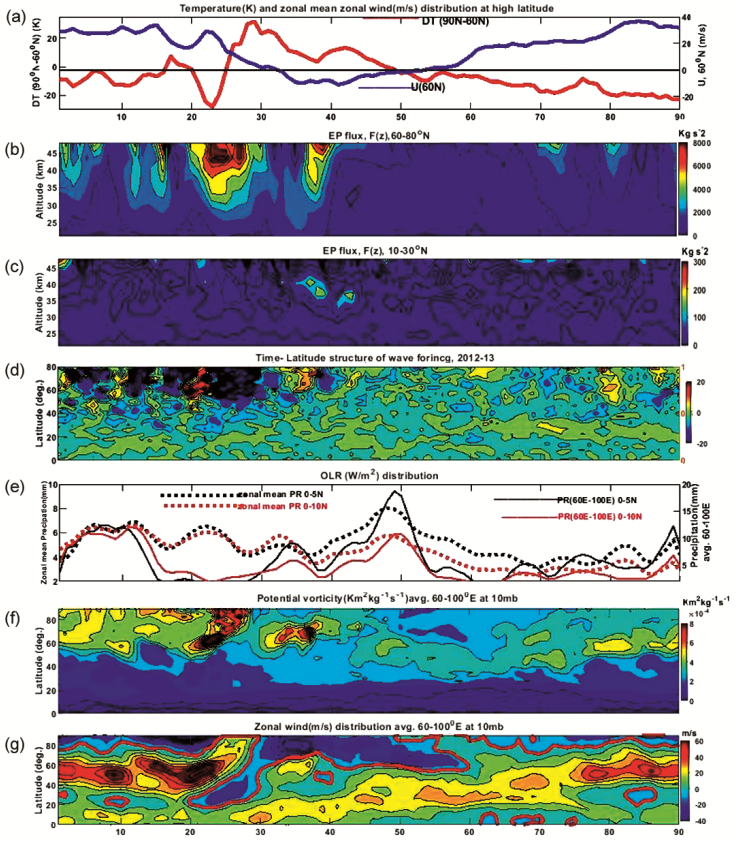


Fig. 5 — The same parameters as Figure 1 but for the 90 days of winter 2018/19 from 01 December 2018.

trend returns to a cold state at the end of January 2019. From the zonal mean wind profile at 60°N, the eastward wind starts to descend on 23 December 2018 on 02 January 2019 (day no. 33); the winds turn westward, and this reversed westward wind exists till 22 January 2019 (day no. 53), become eastward on 23 January 2019 (day no. 54). From Fig. 5(b), Two bursts of intense heat flux observed between 22 -31 December 2018 (day no: 22 to 31) and 05 January 2019- 10 January 2019 (day no. 36 to 41), both the wave energies reach up to the lower stratosphere. In the low latitude band from Fig. 5(c), a weak heat flux reached the mid-stratosphere on 26 December 2018. The second wave bursts reached firmly up to the lower stratosphere (~32 km) from 04 January 2019- 13 January 2019. The latitudinal structure of wave driving revealed that intense convergence of 1st wave flux reaches up to 19°N around 24 December 2018. Forcing connection with the 2nd burst of wave flux is confined over high latitude. But after the warming, wave energies propagate downward as batches to low latitudes. From Fig. 5(e), the zonal mean precipitation steadily increases and maximizes around 18 January 2019 (day no. 49) Whereas, the precipitation averaged over the Indian region shows two maxima on 03 January 2019 (day no. 34) and 18 January 2019 (day no. 49). Strong potential vorticity associated with the wave bursts observed over high latitudes at the time of warming. The extent of potential vorticity distribution is confined within the high and mid-latitudes from Fig. 5 (f). As we can infer from Fig. 5(g), the downward progression of strong westward wind from polar latitudes reached up to 12°N around 23 December 2018, and a weak eastward wind persists near the equator.

### 3.6 Tropical convection during MSW

#### *3.6.1 Total Precipitation during MSW from IMDAA Reanalysis*

Figure 6 shows the total precipitation averaged over 60-100°E for the latitude band 0-5°N (black line) and 0-10°N (red line) for all the winters. To add to the objective of this study, we have taken total precipitation from IMDAA reanalysis as a proxy, along with OLR from NOAA. In the 2003/04 winter, a rise in total precipitation was seen around 24 December 2003 and continued till the end of January. It may be due to the entry of wave flux from high to low latitude and persists till 19 January 2004 (day no: 50). During 2005/06, On 30 December 2005, total precipitation started to increase and reached its maximum on 10 January 2006 (day no:40) and the secondary peak was observed in the mid of February 2006. During the 2008/09 winter, the total precipitation shows a rise around the middle of January in connection with the entry of heat flux from high latitudes. For the winter 2018/19, maximum total precipitation was observed in the beginning and mid-January in connection with wave flux. We infer that entering planetary wave energy to the low latitude band increases the tropical convection by increasing precipitation/ decreasing OLR.

#### *3.6.2 Zonal mean OLR during MSW*

Figure 7 depicts the latitudinal variation of zonally averaged three-day mean OLR for the winters 2003/04, 2005/06, 2008/09, 2012/13, and 2018/19. The convection changes during MSW are explained by selecting the day events are (i) onset of warming, (ii) peak temperature condition, (iii) wind reversal state, and (iv) wind recovery state expressed as a departure from that of before warming state. Zonal mean OLR is a function of the latitude for the selected events. To illustrate the evolution during MSW, OLRs are represented as a departure from the pre-warming state. For the winter of 2003/04, the appointed days are 15, 28 December 2003, 05, and 17 January 2004 as a departure from 10 December

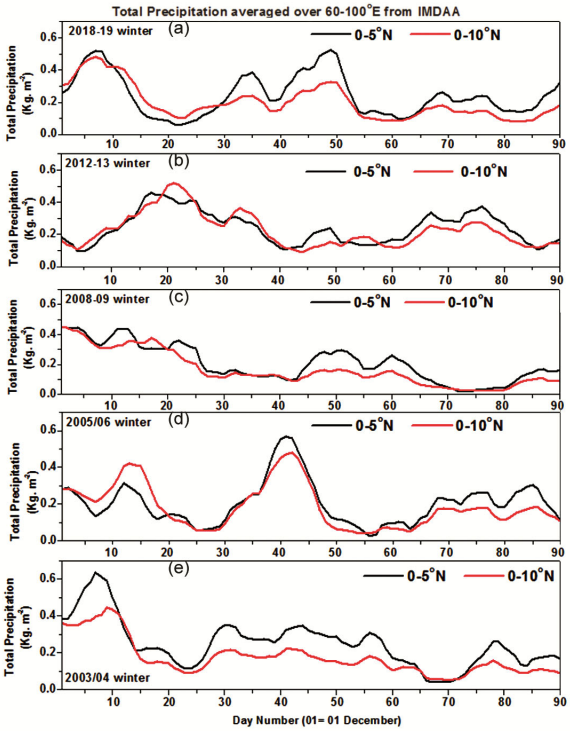


Fig. 6 — Temporal variation of total precipitation averaged over 60-100°E for the latitude band 0-5°N and 0-10°N for all winters.

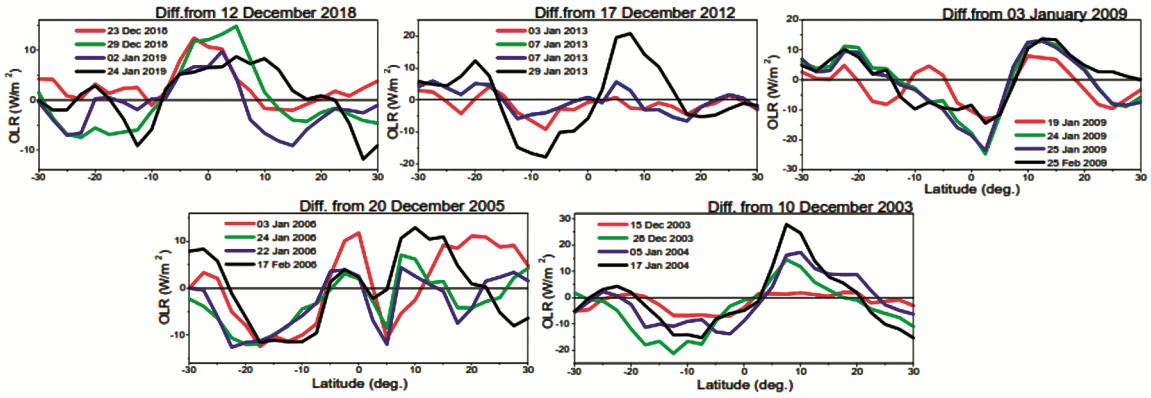


Fig.7 — The latitudinal structure of zonally averaged three days mean OLR during MSW.

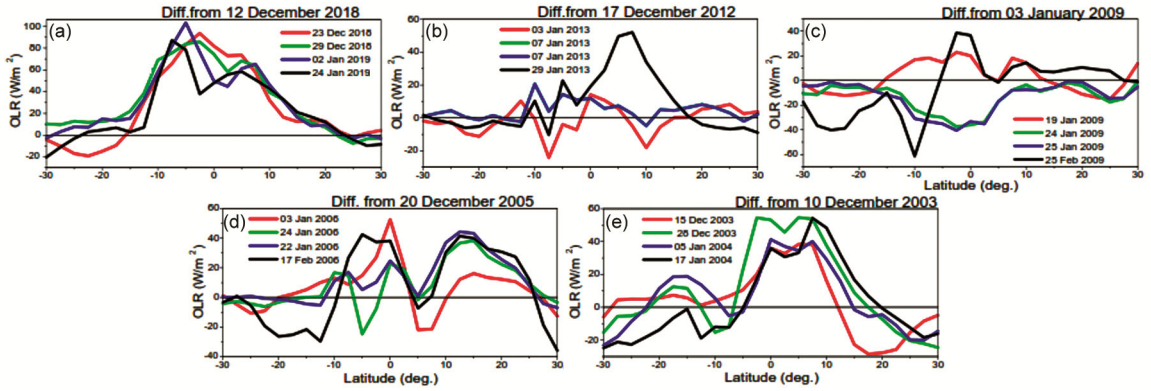


Fig. 8 — Latitudinal structure three days mean OLR averaged over 60-100°E during MSW.

2003. The date indicates the central day of the three-day mean. The seesaw pattern between north and south grows from the initial stage. The maximum negative deficit of OLR (high convection) occurs at the peak temperature stage over low southern latitudes. In contrast, the maximum positive deficiency of OLR (intense convection) occurs at the wind recovery stage over low northern latitudes. In 2005/06, the selected day events 03, 24, 22 January 2006, and 17 February 2006 are exhibited as departures from 20 December 2005. The maximum negative deficit of OLR (high convection) occurs at the peak temperature stage over low southern latitudes. The abrupt drop of OLR (Increased convection) occurs at the onset, peak temperature, and the wind reversed stage over low northern latitudes. For the winter of 2008/09, the days 19, 24, 25 January, and 25 February 2009 were selected as departures from 03 January 2009. Distinct from winter 2003/04 and 2005/06, the OLR deficit progressed near the equator during MSW, maximum negative deficiency occurred at peak temperature, and the wind reversed stage. At 2012/13 MSW, 03, 07, 07, and 27 January 2013 are revealed as departures from 17 December 2012. The maximum positive (negative) OLR deficit occurs at the wind recovery stage (27 January 2013) over the northern (southern) low latitudes. In the 2018/19 MSW case, the selected days are 23, 29 December 2018, 02, and 24 January 2019 as a departure from 12 December 2018. The maximum positive deficit of OLR (low convection) was observed at the peak temperature stage over the equator. The maximum negative OLR deficit occurs at the wind-reversed stage over the southern low latitudes. The OLR trend observed in 2018/19 shows the reverse behaviour of winter 2008/09. As we can infer from Fig. 7, there is evidence of depleted convection in the latitude band 0-20°N for the winters 2003/04, 2008/09, and 2012/13. The winters 2005/06 and 2018/19 show an abrupt change in zonal mean OLR activity in the latitude band 0-20°N.

### *3.6.3 OLR during MSW over Indian region*

Figure 8 illustrates the modulation of tropical convection averaged over the Indian region during

mid-winter stratospheric warming. Fig. 8 depicts the latitudinal structure of 60-100°E averaged three-day mean OLR for the winters 2003/04, 2005/06, 2008/09, 2012/13, and 2018/19. The convection changes during MSW are explained by selecting the day events are (i) onset of warming, (ii) peak temperature condition, (iii) wind reversal state, and (iv) the wind recovery state expressed as a departure from that of before warming state. The longitude 60-100°E averaged OLR is a function of the latitude for the selected events. To illustrate the evolution during MSW, OLRs are displayed as a departure from the pre-warming state. For winter 2003/04, the selected days are 15, 28 December 2003, 05, and 17 January 2004 as a departure from 10 December 2003. The date indicates the central day of the three-day mean. The abrupt seesaw pattern between north and south grows from the initial stage. The small positive deficit of OLR (low convection) occurs during warming over southern low (-10°S-20°S) latitudes. In contrast, the maximum positive shortfall of OLR (intense convection) occurs in the latitude band -5°-15°N at the time of major warming. In 2005/06, the selected day events 03, 24, 22 January 2006, and 17 February 2006 are exhibited as departures from 20 December 2005. The abrupt drop of OLR (Increased convection) occurs at the onset, peak temperature, and the wind reversed stage in the latitude band 0-10°N. The maximum deficit of convection was seen during the warming in the latitude band 10-20°N. Fluctuating up and down variations are seen in OLR when peak temperature and wind reversal stage. For the winter of 2008/09, the days 19, 24, 25 January, and 25 February 2009 were selected as departures from 03 January 2009. Distinct from winter 2003/04 and 2005/06, a negative deficit of OLR (increased convection) was observed in the equatorial band 20°S-20°N at peak temperature, and the wind reversed stages.

Further, Enhanced convection was observed over latitude band 10°S-10°N at the time of warming. The varying convective activity was found at the onset and recovery stage of warming. In the winter of 2012/13, a sudden drop in OLR was observed at the onset of warming. But, during the course and end of warming, a significant short of convection occurs in the latitude band 10°S-10°N. In the 2018/19 MSW case, the selected days are 23, 29 December 2018, 02, and 24 January 2019 as a departure from 12 December 2018. The positive deficit of OLR (low convection) was observed at all stages of warming in the latitude band -15°S-20°N. The OLR trend observed in 2018/19 is distinct from other winters, i.e., equatorial convective activity drastically reduced in all warming stages. The winter 2018/19 response is similar to winter 2003/04. As we can infer from Fig. 8, there is evidence of depleted convection in the latitude band -15-20°N for the winters 2003/04 and 2018/19. The winter of 2012/13 and 2005/06 shows rapid changes in the OLR. The winter of 2008/09 showed enhanced convection in the entire latitude band 20°S-20°N. The present work confirms Kodera and Yamada[16], and Kodera[9].

## 4 Discussion

Using Observations over the Indian Continent, Resmi *et al*.[28] revealed an intense cooling of order 10-15 °C during the peak phase of warming in the entire tropics (30°N -30°S) associated with SSW by investigating the winters 1984-85, 1987-88, 1998-99, and 2008-09. Further, their study again confirms the coupling between the low and high latitudes associated with SSWs. Kodera and Yamada[16] examined the tropical lower-stratospheric response to sudden stratospheric warming in the Southern Hemisphere in September 2002. Besides, this major warming in September 2002 produced a north-south sea saw convective activity. Thuburn and Craig[29] demonstrated that the stratospheric meridional circulation change could affect the diabatic heating rate of convection in the equatorial troposphere. Quanliang Chen *et al*.[30] completed a considerable study by taking 52 sudden stratospheric warming events from 1957 to 2002 to investigate the impact of the East Asian Winter Monsoon (EAWM). They found significant cooling over coastal East Asia centred over Japan, whereas warming over East Asian Inland. The upward propagating planetary waves in the polar stratosphere before the event of SSW lead to a decrease in the stratospheric circumpolar eastward winds.

During major warming episodes, Sivakumar *et al*.[8] and Charyulu *et al*.[31] showed planetary wave propagation from high to mid to low latitudes. Further, Bhagavathiammal *et al*.[32] evidenced that PW flux reaches much lower latitudes during the boreal event than during the austral event. Further, Bhagavathiammal[33] shows the significant changes in tropical weather like convection, temperature, and wind circulation during vortex split major

stratospheric warming events utilizing three events 1984-85, 1988-89, and 2008-09. Using Eliassen-Palm diagnostics, Koushik *et al*.[34] reported that tropical stratopause acts as a precursor for sudden stratospheric warmings using Eliassen Palm flux diagnostics. They identified enhanced planetary wave driving around the tropical stratopause and poleward progression of zero wind line as early indicators for SSW events. Enhanced planetary wave activity undergoes wave breaking, leading to high potential vorticity stratospheric air into the tropical upper troposphere[35]. In addition, PV intrusions to the tropics are linked to tropical convection[36]. Kodera *et al*.[37] investigated the role of deep convection and overshooting convective clouds in the tropics during sudden stratospheric warming in 2009 and 2010. The equatorial southern hemisphere showed an increment of convective activity and precipitation in the winter of 2009 and 2010 due to the strengthening of the Brewer-Dobson Circulation induced by enhanced stratospheric planetary wave activity. Kodera[9] examined the stratosphere's role in equatorial convection by analyzing twelve stratospheric warmings from 1979 to 2001. They suggested that the meridional circulation change associated with stratospheric warming produces lower tropical UT-LS temperature and leads to a pattern of seesaw convective activity in the equatorial troposphere. Further, their analysis concludes enhanced convection near the low latitude southern hemisphere ($10^oS$ - Equator) and suppressed convection near the northern hemisphere ($5^oN$-$15^oN$).

## Conclusions

The present work concludes the impact of mid-winter stratospheric warming on tropical convection over the Indian longitudes. The study utilizes the recent five Mid-winter Stratospheric Warming (MSW) events in the winters 2003/04, 2005/06, 2008/09, 2012/13, and 2018/19 from ECMWF ERA-Interim reanalysis, Outgoing Longwave Radiation (OLR) data from NOAA, and Precipitation from TRMM and IMDAA. We infer from this study that in all mid-winter cases, the forcing of extratropical planetary waves dominates throughout the stratospheric warming process. The downward propagation of vertical heat flux indicates that the transfer of PW energy from high to low latitudes with a few days' delay further modifies the convection pattern. The latitudinal structure of OLR during MSW once again confirms the seesaw pattern between north and south grows from the initial stage. The abrupt drop of OLR (Increased convection) occurs at the onset, peak temperature, and the wind reversed stage over low northern latitudes. The zonal mean structure of OLR suggests that the winters 2003-04, 2008-09, and 2012-13 reveal the depleted convection, but winters 2005/06 and 2018/19 show an abrupt OLR change over the latitude band $0$-$20^oN$. The OLR pattern averaged over Indian longitudes shows depleted convection in the latitude band $-15$-$20^oN$ for the MSW 2003/04 and 2018/19. In the case of MSW, 2012/13 and 2005/06 show rapid changes in the OLR. But, The MSW 2008/09 show enhanced convection in the entire latitude band $20^oS$-$20^oN$. Henceforth, This study suggests that modification of OLR depends on the entry of PW energy, time of onset, peak temperature, and the wind-reversed state of MSW. Including more mid-winter case studies will help us understand the connection between Mid-winter stratospheric warming and tropical convection.

## Conflict of Interests

The authors declare that there is no conflict of interest regarding the publication of the paper.

## Acknowledgements

This work was supported by the Science and Engineering Research Board (SERB), Department of Science and Technology, New Delhi, under the Early Career Research Award (ECR) Scheme[Grant No: ECR/2016/001751]. In addition, The author thanks ECMWF ERA-Interim reanalysis, NOAA Climate Data Centre, and NASA TRMM mission. The author gratefully acknowledges NCMRWF, the Ministry of Earth Sciences, Government of India for IMDAA reanalysis. IMDAA reanalysis was produced under the collaboration between the UK Met Office, NCMRWF, and IMD with financial support from the Ministry of Earth Sciences under the National Monsoon Mission programme.

## References

1 Matsuno T, *J Atmos Sci,* 28 **(**1971**)** 1479.
2 Liu H L & Roble R G, *J Geophys Res,* 107 (2002) 4695.
3 Limpasuvan V, Thompson D W J & Hartmann D L, *J Clim*, 17 (2004) 2584.
4 Fritz S & Soules S D, *J Atmos Sci,* 27 **(**1970**)** 1091.
5 Mukherjee B K & Ramana M B V, *Monthly Weather Review,* 100 **(**1972**)** 674.
6 Dunkerton T, Hsu C P F & McIntyre M E, *J Atmos Sci,* 38 **(**1981**)** 819.
7 Mukherjee B K, Indira K & Dani K K, *Meteorol Atmospheric Dynamics*, 37 **(**1987**)** 1.

8 Sivakumar V, Morel B, Bencherif H, Baray J L, Baldy S, Hauchecorne A & Rao P B, *Atmos Chem Phys*, 4 (2004) 1989.
9 Kodera K, *Geophys Res Lett*, 33 (2006) L06804.
10 Shepherd M G, Wu D L, Fedulina I N, Gurubaran S, Russell J M, Mlynczak M G & Shepherd G, *J Atmos Solar-Terr Phys,* 69 (2007) 2309.
11 Holton J R, Haynes P H, Mclntyre A R, Douglass, Rood R B & Pfister L, *Rev Geophys,* 33 **(**1995**)** 403.
12 Eguchi N & Kodera K, *SOLA,* 6 (2010) 137.
13 Kodera K, Eguchi N, Lee J N, Kuroda Y & Yukimoto S, *J Meteorol Soc Jpn,* 89 **(**2011**),** 283.
14 Yoshida K & Yamazaki K, *Atmos Chem Phys Discuss,* 11 (2011) 2263.
15 Eguchi N, Kodera K & Nasuno T, *Atmos Chem Phys,* 15 (2015) 297.
16 Kodera K & Yamada K, *Meteorol Geophys*, 54 (2004) 115.
17 Kuroda Y, *J Geophys Res,* 113 (2008) D15110.
18 Sridharan S & Sathishkumar S, *J Atmos Sol Terrestr Phys*, 73 (2011) 2453.
19 Harada Y, Goto A, Hasegawa H, Fujikawa N, Naoe H & Hirooka T, *J Atmos Sci,* 67 (2010) 2052.
20 Indira R S, Arulalan T, John P George, Rajagopal E N, Renshaw R, Adam Maycock, Dale Barker & Rajeevan M, *J Climate*, 34 (2021) 5109.
21 Liebmann B & Smith C A, *Bull Am Meteorol Soc,* 77 **(**1996) 1275.
22 Andrews D G & McIntyre M E, *J Atmos Sci,* 33 (1976) 2031.
23 Andrews D G & McIntyre M E, *J Fluid Mech,* 89 (1978) 609.
24 Andrews D G, Leovy C B & Holton J R, *Midd Atmospheric Dynamics*, 40 (1987) 489.
25 Edmon H J, Hoskins B J & McIntyre M E, *J Atmos Sci,* 37 (1980) 2600.
26 Eliassen A & Palm E, *Geofys Publ,* 22 (1961) 1.
27 Sato Y, *J Meteor Soc Jpn*, 58 (1980) 430.
28 Resmi E A, Mohanakumar K & Appu K S, *J Atmos Solar-Terr Phys,* 105-106 (2013) 15.
29 Thuburn J & Craig G C, *J Atmos Sci,* 57 (2000) 17.
30 Quanliang C, Luyang X & Hongke C, *Adv Meteorol*, 640912 (2015).
31 Charyulu D V, Sivakumar V, Hassan B, Guillaume K, Alain H, *et al*., *Atmospheric Chem Phys Discuss*, 7 (2007) 15739.
32 Bhagavathiammal G J, Sathishkumar S, Sridharan S & Gurubaran S, *J Atmos Solar-Terr Phys,* 146 (2016) 205.
33 Bhagavathiammal G J, *Dynamics Atmospheres Oceans*, 101146 (2020).
34 Koushik N, Kishore Kumar K & Pramitha M, *Sci Rep*, 12 (2022) 2937.
35 Waugh D W & Polvani L M, *Geophys Res Lett,* 27 (2000) 3857.
36 Kiladis G N, *J Atmos Sci,* 55 (1998) 321.
37 Kodera K, Funatsu B M, Claud C & Eguchi N, *Atmos Chem Phys*, 15 (2015) 6767.